Chemistry and Physics of Lipids 221 (2019) 120–127

Contents lists available at ScienceDirect

Chemistry and Physics of Lipids

journal homepage: www.elsevier.com/locate/chemphyslip

Rational selection of reverse phase columns for high throughput LC–MS lipidomics

Angela Criscuolo[a,b,c], Martin Zeller[c], Ken Cook[d], Georgia Angelidou[a,b], Maria Fedorova[a,b,*]

[a] Institute of Bioanalytical Chemistry, Faculty of Chemistry and Mineralogy, University of Leipzig, Germany
[b] Center for Biotechnology and Biomedicine, University of Leipzig, Germany
[c] Thermo Fisher Scientific (Bremen) GmbH, Hanna-Kunath-Str. 11, 28199, Bremen, Germany
[d] Thermo Fisher Scientific, Stafford House 1 Boundary Park, HP2 7GE, Hemel Hempstead, United Kingdom

ARTICLE INFO

Keywords:
Lipidomics
Reverse-phase liquid chromatography
LC–MS
Blood plasma

ABSTRACT

Natural lipidomes are characterized by extremely high complexity and dynamic range of lipid concentrations. Furthermore, high diversity of lipid physicochemical properties requires high resolving powers for both chromatographic and mass spectrometric analytical platforms. Reverse-phase chromatography coupled with data-dependent MS/MS acquisition is one of the most popular techniques in untargeted lipidomics. Optimal method should provide good chromatographic separation and resolution, reproducibility, selectivity and sensitivity. Here, we developed and set-up a RPLC-MS/MS workflow capable of resolving complex mixtures of lipids in 32 min of analysis. Human blood plasma was chosen as a representative complex natural lipidome with large variance of lipid classes, species and lipid concentrations. Lipids were separated by RPLC on five different reverse phase columns with different types of stationary phase particles, size and chemistry. High mass accuracy MS analysis and data-dependent MS/MS analysis were performed using a Q Exactive™ HF Hybrid Quadrupole-Orbitrap™ Mass Spectrometer to identify individual lipid molecular species. This workflow was applied to evaluate the separation capability of each column and to identify the lipidomics profile in highly complex biological samples. As a result, we report more than 600 lipid species covering 18 lipid classes in human blood plasma and provide suggestions to the selection of the appropriate reverse phase column for the analysis of specific lipidomes.

1. Introduction

Lipids are involved in a wide range of biological function including compartmentalization via biological membranes, energy storage, signaling, transport control, and regulation of inflammation, to name just a few. Such functional diversity and associated degree of specialization are mainly determined by a high variety of lipid physicochemical properties and complexity of natural lipidomes. Currently, the number of entries reported in various databases include from tens to hundreds of thousands of lipid species. For instance, LIPID MAPS database reports more than 43,000 lipid structures derived from experimental data as well as computationally predicted ones. Despite the large number of lipid entries in various databases, numbers of lipids reliably identified in biological samples usually do not exceed 500 molecular species identified at fatty acyl level. Recent studies demonstrated that mass spectrometry based lipidomics, which is the large-scale study of diversified molecular species of lipids, aiming to address the identification, cellular and tissue distribution of lipids as well as related signaling and metabolic pathways, has a very high potential in defining the diversity of natural lipidomes.

Abbreviations: ACN, acetonitrile; a.u., arbitrary units; Cer, ceramides; CE, cholesteryl ester; Co, coenzyme; DDA, data dependent acquisition; DG, diglyceride; DMPE, dimethylphosphatidylethanolamine; FA, free fatty acid; FPP, fully porous particles; IPA, isopropano; lLC, liquid chromatography; LPA, lysophosphatidic acid; LPC, lysophosphatidylcholine; LPE, lysophosphatidylethanolamine; LPG, lysophosphatidylglycerol; LPI, lysophosphatidylinositol; LPL, lysophospholipids; LPS, lysophosphatidylserine; MeOH, methanol; MG, monoglyceride; MTBE, tert-methyl-butyl ether; N, number of theoretical plates; PA, phosphatidic acid; Pc, peak capacity; PC, phosphatidylcholine; PE, phosphatidylethanolamine; PG, phosphatidylglycerol; PI, phosphatidylinositol; PL, phospholipids; PS, phosphatidylserine; R, chromatographic resolution; Rt, retention time; S/N, signal to noise ratio; SCP, solid core particles; SiE, sitosterol ester; SM, sphingomyelin; ST, sulfatide; TG, triglyceride; W, peak width at the baseline; WE, wax ester

* Corresponding author at: Institut für Bioanalytische Chemie, Faculty of Chemistry and Mineralogy, Biotechnologisch-Biomedizinisches Zentrum, Leipzig University, Deutscher Platz 5, 04103, Leipzig, Germany.
E-mail address: maria.fedorova@bbz.uni-leipzig.de (M. Fedorova).

https://doi.org/10.1016/j.chemphyslip.2019.03.006
Received 30 January 2019; Received in revised form 7 March 2019; Accepted 14 March 2019
Available online 30 March 2019

Table 1
Characteristics of the five RP column used in the study.

Column	Accucore C18	Hypersil GOLD C18	Accucore C30	Acclaim C30 1.9 µm	Acclaim C30 3.0 µm
Phase	Silica, Spherical Solid Core Ultrapure	Silica, Spherical Fully Porous Ultrapure	Silica, Spherical Solid Core Ultrapure	Silica, Spherical Fully Porous Ultrapure	Silica, Spherical Fully Porous Ultrapure
Chemistry	C18	C18	C30	C30	C30
Particle size	2.6 µm	1.9 µm	2.6 µm	1.9 µm	3.0 µm
Pore size	150 Å	175 Å	150 Å	120 Å	200 Å
Surface area	80 m^2/g	220 m^2/g	90 m^2/g	175 m^2/g	200 m^2/g
Carbon load	7%	11%	5%	~10% (estimate)	13%
End capped	Yes	Yes	Yes	Yes	Yes
pH range	2-8	1-11	2-8	2-8	2-8
Length	150 mm	150 mm	150 mm	150 mm	250 mm
Maximum backpressure	1000 bar	1250 bar	1000 bar	1250 bar	690 bar
Maximum operating temperature	70 °C	60 °C	70 °C	60 °C	60 °C
Optimal flow rate	0.4 mL/min	0.5 mL/min	0.4 mL/min	0.5 mL/min	0.2-0.3 mL/min
Operating back pressure	250 – 360 bar	380 – 620 bar	250 – 360 bar	380 – 560 bar	240 – 370 bar

Discovery or untargeted mass spectrometry (MS)-based omics techniques, including proteomics, metabolomics and lipidomics, aim for the identification of as many as possible (preferentially "all") individual molecular species present in the sample, and usually rely on LC–MS based data dependent acquisition (DDA) methods. For optimal performance and to assure highest "-ome" coverage, both LC and MS methods require careful optimization. Nowadays, limitations associated with DDA "undersampling" are at least partially solved by the introduction of high mass accuracy and high (spectral) resolution mass analyzers operating at a high speed to provide the large number of individual MS/MS scans necessary to identify molecular species. On the other hand, LC separation can be further optimized in order to ensure the best capacity, selectivity and sensitivity of the whole analytical workflow.

In lipidomics, and to a larger extent in metabolomics, extremely high physicochemical diversity of analytes represents one of the main analytical challenges (Shevchenko and Simons, 2010). Lipids are represented by eight categories which include fatty acids, glycerolipids, glycerophospholipids, sphingolipids, sterol lipids, prenol lipids, saccharolipids, and polyketides. These different groups differ in their logP (hydrophobicity) values by several orders of magnitude (Lange et al., 2019). Thus optimization of experiments aiming to cover complex biological lipidomes requires not only tuning of MS acquisition parameters, but also efficient lipid extraction and separation strategies (Burla et al., 2018; Cajka and Fiehn, 2014; Hu and Zhang, 2018). Furthermore, the high dynamic range of lipid concentrations in complex biological samples (Li et al., 2014) (e.g. human blood or adipose tissue) requires high peak capacity and selectivity of the separation method. Moreover, the presence of a high number of isobaric and isomeric species is an additional challenge for the LC separation to aid in the identifications. Reversed-phase liquid chromatography (RPLC), one of the most popular separation techniques in lipidomics (Hu et al., 2008; Lange et al., 2019; Martano et al., 2015; Rainville et al., 2007; Sandra et al., 2010), provides separation of lipids based on the hydrophobicity of their fatty acyl chain moieties and thus can separate lipids based on the length of fatty acid chains, number and potentially positions of the double bonds (Ovčačíková et al., 2016). Optimal RPLC - MS methods should have high peak capacity, chromatographic resolution, reproducibility, selectivity and sensitivity. Furthermore, the separation has to be compatible with the DDA cycle on a new generation of MS instruments allowing acquisition of tandem mass spectra for the high dynamic range of lipid concentrations. Application of sub-2 µm fully porous particles (FPP) found wide application in lipidomics profiling due to the highly efficient, fast and robust separation of complex lipid samples (Witting et al., 2014). Alternatively, solid core particles (SCP) were reported to provide similar efficiency without generating the high backpressure associated with sub-2 µm FPP (Bird et al., 2012; Narváez-rivas and Zhang, 2016). The choice of stationary phase chemistry for lipid separation includes C8, C18 and C30 RP columns of which the longer chain C30 phase provides greater selectivity for the large hydrophobic fatty acyl chains and results in higher resolution of structurally close lipid isomers (Narváez-rivas and Zhang, 2016; Rampler et al., 2017). In RPLC, selectivity of the separation is primary based on the hydrophobicity of the analytes. The hydrophobicity of the stationary phase depends mostly on the hydrocarbon moiety and the amount which is bonded onto the chromatography resin particle. This is generally reflected by the length of the stationary phase-bounded alkyl chains. RPLC stationary phases with longer alkyl chains (C18 and C30) provide better recognition and align better with long chain hydrophobic analytes (lipids) improving the selectivity of closely related lipid species (Narváez-rivas and Zhang, 2016; Vyňuchalová and Jandera, 2015).

Here, we compared in terms of efficiency, selectivity and chromatographic resolution five RP columns with different types of stationary phase particles (FPP vs. SCP), size (1.9 µm vs. 2.6 µm vs. 3.0 µm) and chemistry (C18 vs. C30) using a unique elution gradient and MS method. Where possible the chemistry of the particles were kept the same to allow conclusions to be drawn that are based on comparisons of specific differences in the resins. The designed method was based on a relatively short gradient elution of 26 min, with a total analysis time after column equilibration of 32 min. Application of different RP columns in LC–MS experiments provided identification of more than 600 individual lipid species in human blood plasma and allowed us to formulate a recommendation on RP columns selection strategy based on the lipidome diversity.

2. Material and methods

2.1. Chemicals and columns

Acetonitrile, isopropanol, water, methanol, *tert*-methyl-butyl ether (MTBE) (Optima LC–MS grade) and chloroform (LC–MS grade) were obtained from Fisher Scientific (Schwerte, Germany). Ammonium formate, formic acid (LC–MS grade) and human plasma were purchased from Sigma-Aldrich (Sigma-Aldrich, Munich, Germany). HPLC columns (Table 1) were supplied by Thermo Fisher Scientific (Sunnyvale, CA, USA). The Acclaim C30 with 1.9 µm is still a prototype column and not yet available on the market.

2.2. Lipid extraction from human blood plasma

Lipids from human blood plasma (40 µL) were extracted following the MTBE extraction protocol (Matyash et al., 2008). MTBE extracts were dried and re-dissolved in methanol (400 µL) prior to the injection.

2.3. Chromatographic conditions

UHPLC separation was performed on Thermo Scientific™ UltiMate™ 3000 UHPLC System equipped with a binary pump, an autosampler and a column compartment. A binary solvent system was used, in which eluent A consisted of acetonitrile:water, (50:50, v/v) and eluent B of isopropanol:acetonitrile:water, (85:10:5, v/v), both containing ammonium formate (5 mmol/L). Separations were carried out following the conditions set by Rampler et al. (Rampler et al., 2017). Lipids (5 µL in methanol; each sample in technical triplicate) were loaded onto a reverse phase columns (Table 1) at 25% B and eluted using several gradient steps: ramp from 25% to 86% B (20 min; non-linear slop curve 4), 90% (2 min), 95% (2 min), and isocratic gradient at 95% (2 min). Together with an equilibration time of 6 min the samples were injected every 32 min. Column temperature was set to 50 °C and the flow rate to 325 µL/min.

2.4. Mass spectrometry

A Thermo Scientific™ Q Exactive™ HF Hybrid Quadrupole-Orbitrap™ Mass Spectrometer using a Thermo Scientific™ HESI Source was operated in data-dependent acquisition (DDA) mode. Lipids were analyzed in separate runs in both positive and negative ion modes. Ion source voltage was set to 3.5 kV (positive mode) or -3.0 kV (negative mode), ion transfer tube temperature was 230 °C; sheath, aux, and sweep gases were set to 45, 15 and 1 arbitrary units, respectively. Vaporizer temperature was 370 °C. The S-Lens RF level was set to 35%. The Orbitrap mass analyzer was operated at a resolution setting of 120,000 (at *m/z* 200) in full-scan mode (scan range: 400-1200 *m/z* in positive ion mode, 250-900 *m/z* in negative ion mode; automatic gain control target: 3e6; max. injection time: 100 ms) and at a resolution setting of 30,000 (at *m/z* 200) in the Top10 DDA MS/MS mode (HCD, Stepped Normalized Collision Energy: 20 ± 10 eV; Isolation Width: 1.2 Da; Activation Q: 0.2; Activation Time: 10 ms; automatic gain control target: 1e5; max. injection time: 150 ms; Intensity threshold: 1e3 counts) with dynamic exclusion for 10 s and in profile mode.

2.5. Lipid identification and data processing

Lipids were identified using LipidSearch™ software version 4.1 SP1 using the following key processing parameters: target database – general, precursor tolerance ± 5 ppm, product tolerance ± 20 ppm, product ion threshold 5%, m-score threshold 1, Quan *m/z* tolerance ± 5 ppm, Quan RT (retention time) range ± 0.5 min, use of main isomer filter and ID quality filters A, B, and C (C - only for PC and SM in positive ion mode). Protonated, sodiated and ammoniated adducts were considered for positive ion mode, and deprotonated and formate adducts were considered for negative ion mode. LPA (lysophosphatidic acid), LPC (lysophosphatidylcholine), LPE (lysophosphatidylethanolamine), LPG (lysophosphatidylglycerol), LPI (lysophosphatidylinositol), LPS (lysophosphatidylserine), ST (sulfatide), PA (phosphatidic acid), PC (phosphatidylcholine), PE (phosphatidylethanolamine), DMPE (dimethylphosphatidylethanolamine), PG (phosphatidylglycerol), PI (phosphatidylinositol), PS (phosphatidylserine), Cer (ceramides), SM (sphingomyelin), MG (monoglyceride), DG (diglyceride), Co (coenzyme), CE (cholesteryl ester), SiE (sitosterol ester), WE (wax ester) lipid classes were selected for the search. For each column, the search results from the 6 individual positive and negative ion mode raw data files (3 for each polarity) and a blank were aligned within a retention time window of ± 9 s and the datasets were merged for each annotated lipid.

Free fatty acids (FA) were not efficiently fragmented under tandem mass spectrometry conditions described above (requires much higher collision energy NCE > 50 eV) and thus the identification was performed manually based on pseudo-molecular ions within mass accuracy window of 3 ppm, for the signals higher than 1e4 counts represented by the peaks with at least four data points.

TG (triglyceride) were identified using LipidHunter software. Raw files where converted to. mzML by using the ProteoWizard 3.0.9134 (Chambers et al., 2012). The converted files were used for the TG identification by LipidHunter version 2.0 (Ni et al., 2017) (https://github.com/SysMedOs/lipidhunter) using the following parameters: scan time range from 20 to 30 min, *m/z* range from 600 to 1200, DDA Top 10, mass accuracy at MS level - 5 ppm, MS intensity threshold - 1e4 counts, mass accuracy at MS/MS level - 20 ppm, MS/MS intensity threshold - 2e3 counts. Identifications were filtered for isotopic score ≥ 75, and rank score ≥ 60.0. The white list of considered fatty acyl chains included 48 fatty acids (from C8 to C26; maximum of six double bonds). Weight Factor list assigned each fatty acid neutral loss fragment ions to 30%, whereas fatty acid and monoacylglycerol fragment ions shared the rest 10%. Identification results were manually confirmed, using a precursor mass tolerance ± 5 ppm, and ALEX^{123} lipid calculator (Pauling et al., 2017).

For evaluation of lipid retention times, peak width at the baseline, peak height, peak area and signal to noise ratio ThermoScientific™ FreeStyle™ 1.3 Software was used.

2.6. Data availability

All raw data are available at https://doi.org/10.17632/7nnxbsszyz.1.

3. Results and discussion

Human blood plasma lipidome was chosen as a complex biological matrix containing over one thousand unique lipid species over a high range of concentrations (e.g. 47% of total content corresponding to cholesteryl esters, and 1% represented by PE) (Bowden et al., 2017) for comparison of five RP columns in their separation efficiencies. The analysis of the plasma lipidome was carried out using a gradient elution over 24.5 min. Considering column dead time of 1.5 min calculated by injecting a non-retaining analyte (alprazolam) and equilibration time of 6 min, total LC–MS analysis was done within 32 min. For each column LC–MS analysis was performed in positive and negative ion modes to ensure highest lipidome coverage.

Each RP column provided a similar elution order with more hydrophilic lipids such as lysophospholipids (LPL) eluting first, followed by free fatty acids (FA), phospholipids (PL), ceramides (Cer), sphingomyelins (SM) and diglycerides (DG). The late eluting compounds were the most hydrophobic lipids - triglyceride (TG) and cholesteryl ester (CE) (Fig. 1). Despite the similar elution order, the more hydrophobic lipids eluted from C18 columns in a very narrow time window whereas on C30 columns, due to their higher retention and selectivity, CEs were well separated from TGs.

The columns performance for LC–MS based lipidomics were compared taking into account several different parameters including the number of identified lipids, peak width, peak capacity, sensitivity, and chromatographic resolution of closely related isomeric lipids.

3.1. Identification of human blood plasma lipidome

Plasma lipids separated by the five different RP columns were analyzed by DDA on Q Exactive HF Hybrid Quadrupole-Orbitrap Mass Spectrometer in positive and negative ion modes and lipid molecular species were identified by LipidSearch software and LipidHunter v.2 (for TGs) software (Ni et al., 2017). Overall, it was possible to identify over 630 lipid molecular species representing 18 lipid classes. The total numbers of identified lipids for each RP column are summarized in the Table 2. All lipid molecular species identified with corresponding *m/z* values and retention times are available in Supplementary Table S1.

Both the Accucore C18 and C30 columns and the 1.9 µm particle size Acclaim C30 column provided the highest numbers of

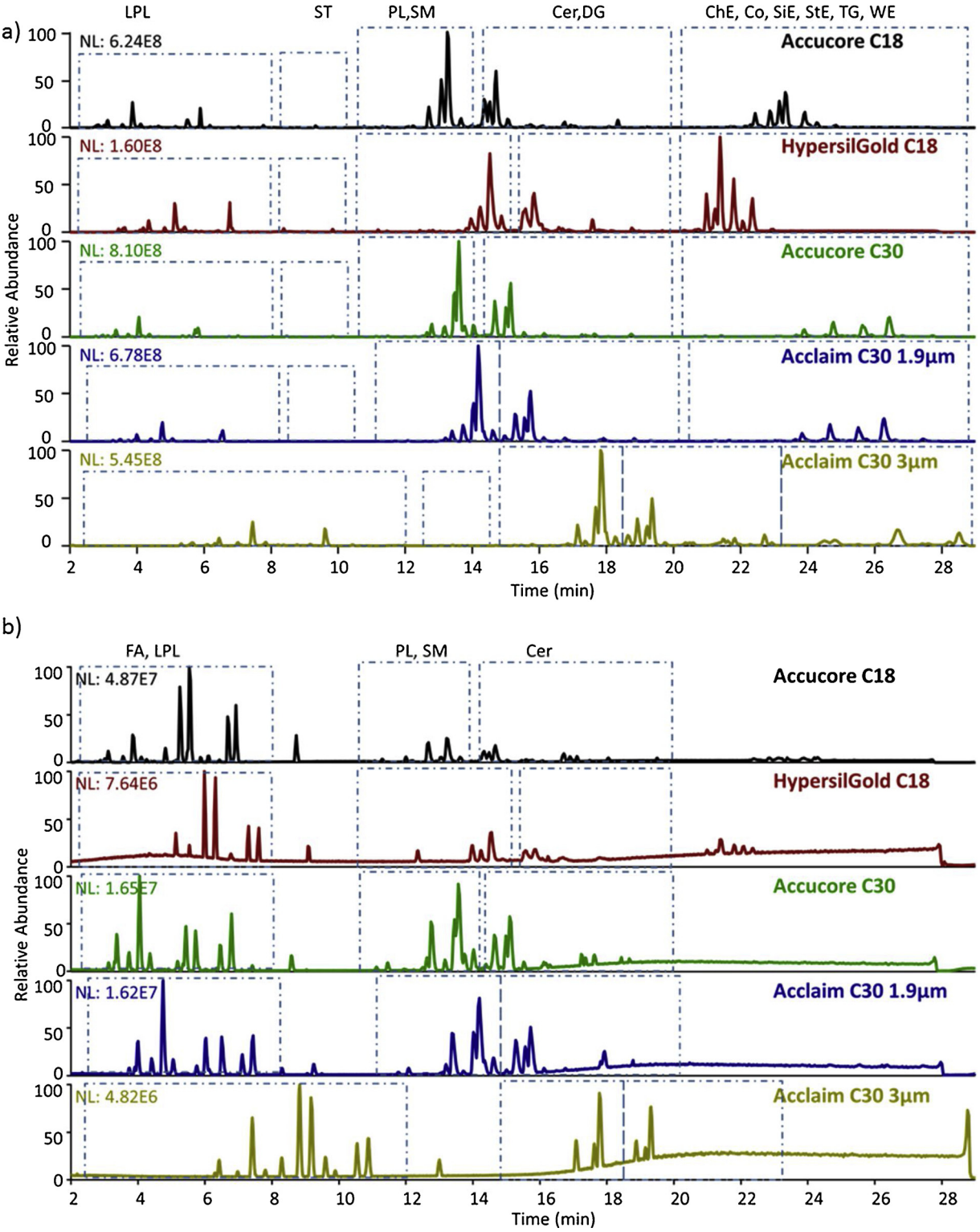

Fig. 1. Basepeak chromatograms of human blood plasma lipidome acquired in positive (a) and negative ion modes (b) using five different RP columns – Accucore C18 (black trace), Hypersil GOLD C18 (red trace), Accucore C30 (green trace), Acclaim C30 with 1.9 µm (blue trace) and 3.0 µm particle size (yellow trace). Boxes illustrate elution time regions for specific lipid classes including FFA, LPL, SM, PL, DG, Cer, CE, Co, SiE, TG, and WE lipids.

identifications (IDs), with some variations within lipid classes as well as a slight difference in the capacity to differentiate isomeric lipids (Table S1). For instance, the highest number of identifications at the lipid species level was provided by Accucore C18 Column [412] whereas highest number of IDs at the fatty acyl level was obtained on the Accucore C30 Column [639]. However, differences in the number of identified species at fatty acyl level between the Accucore columns and 1.9 µm Acclaim columns were very minor. Accucore C18 columns provide the highest number of Lipid Species Level IDs for the majority of lipid classes except PC and PE, and it was also superior in terms of Fatty Acyl Level IDs for free FA, LPLs (except LPC and LPE), DGs, and sphingolipids represented here by ceramides and sphingomyelins. The

Table 2
Number of identifications for lipid species level and fatty acyl level obtained using five RP columns coupled on-line to Q Exactive HF MS operating in DDA mode. Color filled cells correspond to the highest number of lipids identified as a bulk (green) or molecular species (red).

class	Accucore C18		Hypersil GOLD C18		Accucore C30		Acclaim C30 1.9 µm		Acclaim C30 3.0 µm	
	Lipid Species Level ID	Fatty Acyl Level ID	Lipid Species Level ID	Fatty Acyl Level ID	Lipid Species Level ID	Fatty Acyl Level ID	Lipid Species Level ID	Fatty Acyl Level ID	Lipid Species Level ID	Fatty Acyl Level ID
FA	23	28	16	20	22	24	20	22	16	19
LPA	6	6	4	4	0	0	0	0	3	3
LPC	24	39	20	26	23	35	20	33	24	43
LPE	9	11	3	4	6	8	5	7	9	12
LPI	3	3	1	1	1	1	0	0	1	1
ST	2	2	0	0	1	1	1	1	1	1
PC	88	160	63	93	97	174	89	163	83	132
PE	29	43	23	25	31	47	33	53	27	39
PI	18	21	10	10	17	23	18	22	13	15
PS	1	1	1	1	1	1	1	1	1	1
Cer	30	33	17	17	23	25	25	29	22	24
SM	52	77	34	35	50	69	48	65	50	63
DG	20	28	20	24	16	22	19	26	15	19
TG	85	163	72	109	80	183	78	188	75	168
Co	2	3	1	1	2	3	2	3	2	3
CE	16	16	11	11	14	16	15	19	12	14
Sie	1	1	1	1	3	4	2	2	3	3
WE	3	3	2	2	2	3	3	3	2	2
tot	**412**	**638**	**299**	**384**	**390**	**639**	**380**	**637**	**359**	**562**

highest number of lipids within different PL classes were identified by Accucore C30 (PC, PI) column and 1.9 µm Acclaim C30 column (PE). The effect of separation efficiency of isomeric lipid species was best illustrated for hydrophobic lipids such as TG and CE. The Accucore C18 column allowed the highest number of Lipid Species Level IDs for TG [85] and CE [16], however the highest number of identifications for fatty acyl level were obtained after separation of human plasma using the 1.9 µm Acclaim C30 column corresponding to 188 and 19 TG and CE, respectively. Hypersil GOLD C18 column provided the lowest number of IDs, and the Acclaim C30 column with 3.0 µm particle size resulted in an intermediate number of identifications.

Using an identical DDA method for all LC–MS analysis, the difference in the number of identified lipids can be clearly attributed to the separation performance of RP columns determined by their peak capacity, signal intensities, signal to noise ratio as well as chromatographic resolution of critical pairs. To calculate all chromatographic parameters (peak width, peak capacity, sensitivity and chromatographic resolution) we used three to four lipid species (unique *m/z*) with different signal intensities (high, medium and low abundant pseudo-molecular ions; Table S2) from nine main lipid classes (LPC, PC, PE, PI, Cer, SM, DG, TG, CE).

3.2. Chromatographic peak width and column capacity

The width of a chromatographic peak in LC–MS is important since narrow chromatographic peaks result in a chromatographic enrichment increasing method sensitivity. It is particularly crucial for DDA methods where selection of the precursor ions for the fragmentation is based on the ion abundance. Broad chromatographic peaks are translated in lower signal intensity and thus less probability for being selected for HCD fragmentation. For these studies we used the peak width at the baseline. The broadest average peak width (25.0 s) in this study was characteristic for Acclaim C30 column with 3.0 µm particles size, with especially high values for TGs (56.8 s) and CEs (52.3 s). The effect of peak broadening on efficiency of the DDA method for lipidome coverage is evident from the relatively low number of lipid IDs obtained from the Acclaim C30 with 3.0 µm particle size column separation (562 molecular species against the 639 obtained with Accucore C30 column).

All other columns used in the study had an average peak width between 17.2 and 19.4 s, thus providing not only higher sensitivity via chromatographic enrichment but also acquisition of at least two MS/MS scans for each precursor (taking into account the MS duty cycle of 1.6 sec (1 MS and 10 dd-MS2) and dynamic exclusion of 10 s). Indeed, Accucore C18 and C30 columns as well as Acclaim C30 with 1.9 µm particle size provided a high number of unique lipid IDs (Tables 1 and S1). However, the Hypersil GOLD C18 column, despite narrow chromatographic peaks, resulted in the lowest number of IDs, probably due to the low sensitivity signal intensities. This could be due to the low column capacity for lipids derived from a combination of relatively high pore size and surface area (Table1).

3.3. Column separation efficiency and peak capacity

In order to evaluate the efficiency of a column it is common to calculate the Number of theoretical plates (N) using the following equation: $N = 16(Rt/W)$, where Rt corresponds to the retention time, and W to the peak width at the baseline (Martin and Synge, 1941). However, this equation is only valid for isocratic separations and cannot be readily applied to gradient elution (Mayer and Tompkins, 1947). For this reason we used peak capacity to evaluate the efficiency of tested RP columns. The peak capacity (Pc) can be defined as a maximum number of peaks that can be chromatographically separated with a unit resolution within a retention time window (Neue, 2005). We used the equation $Pc = 1 + tg/W$, where tg corresponds to the elution time and W to the average peak width at the baseline (Neue, 2005). Comparable high values for peak capacities were obtained for all tested columns except Acclaim C30 column with 3.0 µm particle size having the lower value (Table 3 and Table S3) due to the broader peaks as mentioned above.

Within different lipid classes the highest peak capacity for LPC as well as PI and SM lipids was displayed by Accucore C30, whereas Acclaim C30 with 1.9 µm particle size had the highest capacity for PC and DG lipids. Interestingly, the Hypersil GOLD C18 column showed the highest capacity for PE, Cer, TGs and CE, despite having lower identification numbers.

Table 3
Comparison of Lipid ID, peak capacity, sensitivity and chromatographic resolution.

	Accucore C18	Hypersil GOLD C18	Accucore C30	Acclaim C30 1.9 µm	Acclaim C30 3.0 µm
Lipid Species Level ID	412	299	390	380	359
Fatty Acyl Level ID	638	384	639	637	562
Peak width, sec	17.2	19.4	17.2	17.1	25.0
Peak capacity, a.u.	96	85	98	94	79
Peak height, counts	2.9e7	8.4e6	2.3e7	2.1e7	1.7e7
Peak area, counts	1.8e8	4.9e7	1.7e8	1.5e8	1.6e8
S/N, a.u.	1.1e5	7.0e4	1.3e5	1.1e5	5.4e4
Chromatographic resolution, a.u.	1.73	0.94	1.93	1.91	1.75

3.4. Sensitivity

The sensitivity relates to the detector signal and the ability of a peak to be seen and chosen for MS/MS. This was evaluated by comparing the peak height, area and the signal to noise ratio (S/N) for the selected analytes with the different columns (Table S2 and S3), considering them as the only variable of the analytical system. Average peak height was the best for Accucore C18 column, followed by Accucore C30, whereas the Hypersil GOLD C18 showed the lowest values. Integrated peak areas for the selected compounds were comparable for all of the columns, except Hypersil GOLD C18 which on average showed at least two times lower values. This concurs with the low sensitivity values of the Hypersil GOLD C18 column and is probably connected with its low capacity for lipids.

S/N ratios were distributed differently for the five tested columns (Table S3). The Accucore C30 column showed the best S/N, especially for phospholipids such as PC and PE, while the C18 columns had higher S/N for the more hydrophobic lipids. It is important to note that chromatographic separation was conducted using a high percentage of isopropanol during the gradient which induced the elution of chemicals backgrounds, mostly at high retention times. Thus the earlier elution times of hydrophobic lipids from C18 columns (corresponding to the lower % of isopropanol) resulted in lower noise, but not in a higher intensity of the signals.

3.5. Chromatographic resolution

The chromatographic resolution for each RP column was calculated using the formula $R = \frac{2(Rt_2 - Rt_2)}{(W_1 + W_2)}$ (IUPAC, 1997) and illustrated for isomeric or structurally close lipids from different classes (Table 3 and S3). Only the Accucore C30 and Acclaim C30 columns were able to differentiate between all chosen species. The Accucore C18 column showed in general good chromatographic resolution, especially for the PE lipids (the chromatographic resolution is at least 20% higher than all the other columns), however it was not able to resolve all the triacylglycerols. This is possibly due to better alignment of the long acyl chains with the C30 ligand compared to a shorter C18 chain length. The Hypersil GOLD C18 column had in general the lowest resolving power for all the examples taken into account. The Accucore C18 column seems to be the best column for the identification of more hydrophilic lipids such as LPL, free FA and sphingolipids, even though it doesn't achieve the best resolving power. The Accucore C30 column provided better identification for phospholipids due to the capability to resolve them well, whereas TGs were in general better resolved by C30 columns, the 1.9 µm particle size Acclaim C30 column showed the highest number of identified species (Fig. 2).

4. Conclusion

Selection of the appropriate reverse phase column for LC–MS analysis of complex natural lipidomes is a key step in method optimization for discovery lipidomics. Lipidomes of different tissues show significant variations in distribution not only of lipid molecular species within one lipid class but also in large variations between the lipid categories.

Here we compared five different RP columns in LC–MS DDA experiments with the aim of providing high identification coverage of lipids in human blood plasma (Table 3). Using RP columns with different surface chemistries (C18 vs C30), types of stationary phase particles (FPP vs. SCP), and their particle size (1.9 µm vs. 2.6 µm vs. 3.0 µm) we can provide recommendations for column selection for lipidomics experiments. This is based on column efficiencies and selectivites for the different lipid classes. Within the five columns used in this comparison, the Hypersil GOLD C18 (FPP with 1.9 µm particle size) showed the lowest values for all analytical parameters tested in the study, probably due to the relatively high pore size and surface area of the stationary phase. This shows that not all C18 columns are efficient for lipid chromatography and selection should not be based entirely on particle size. The Acclaim C30 with 3.0 µm particle size (FPP) provided good chromatographic resolution however it had the lowest peak capacity and sensitivity due to peak broadening, especially at the end of the gradient elution for TGs and CE lipids. The other three columns demonstrated high potential for lipidomics applications by providing the highest number of lipid identifications. Both Accucore columns (SCP) C18 and C30 provided very good peak capacity, sensitivity and chromatographic resolution values. These were closely followed by the Acclaim C30 (FPP, 1.9 µm particle size) column. Furthermore, Accucore C18 performed the best for separation of smaller, relatively polar lipids (LPLs, PLs, Cer, and SM) and thus can be recommended for analysis of lipidomes of intermediate polarity, whereas Accucore C30 and especially Acclaim C30 would be more suitable for samples with a high content of long chain hydrophobic lipids.

Our study based on the comparative analysis of five different stationary phases for reverse-phase separation of complex lipidomes provides recommendation for the rational design of LC–MS/MS experiments. Targeting resolution of multiple lipid species and their identification using DDA.

We also provide identification of more than 600 lipid species covering 18 lipid classes in human plasma lipidome on the fatty acyl level, together with corresponding *m/z* values, types of adducts, and retention times. The raw LC–MS/MS dataset is available at https://doi.org/10.17632/7nnxbsszyz.1. This curated data is available to the community as a reference lipidome to be used in studies related with lipid alterations in human pathologies and for optimization of analytical and computational solutions such as retention time prediction algorithms aiming to improve current lipidomics identification protocols.

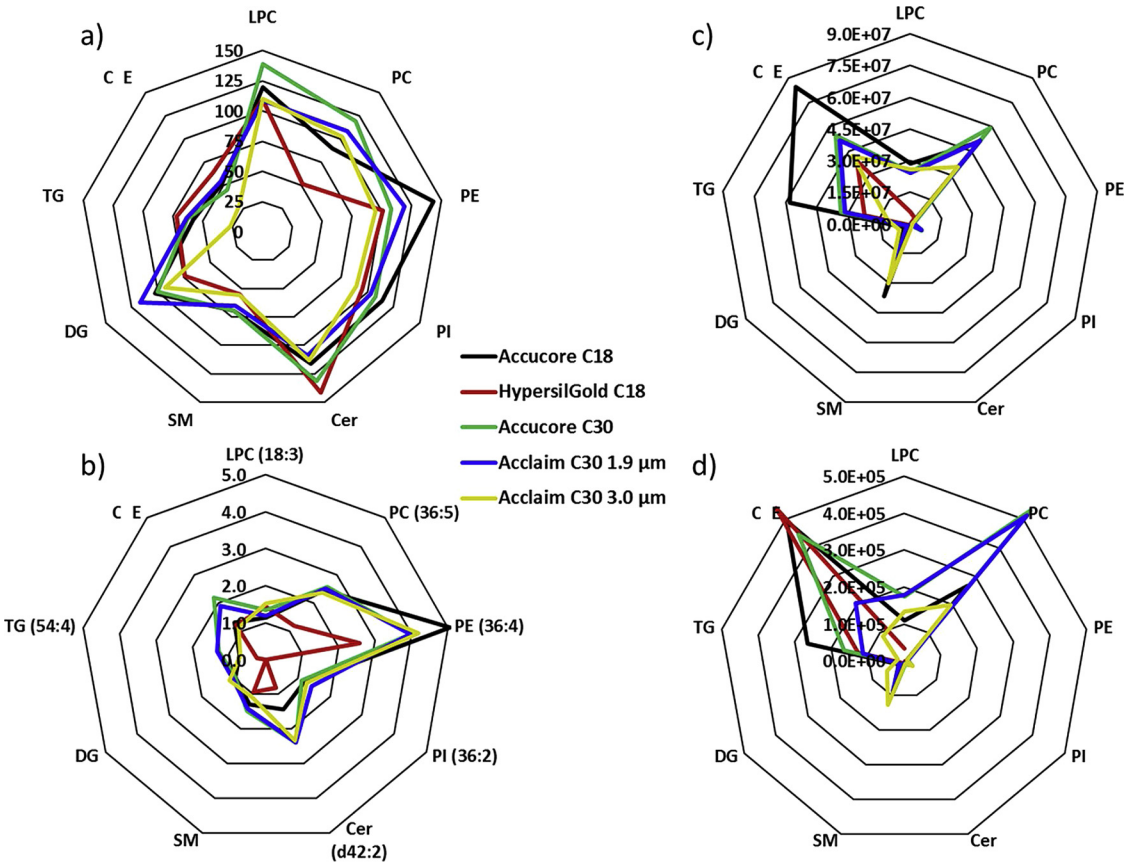

Fig. 2. Pictorial representation of the analytical characteristics tested for the nine lipid classes (LPC, PC, PE, PI, SM, DG, TG, and CE) including (A) average peak capacity (arbitrary units, a.u.), (B) chromatographic resolution (a.u.), (C) peak height (counts), and (D) signal to noise (a.u.). The five different columns represented as Accucore C18 (black trace), Hypersil GOLD C18 (red trace), Accucore C30 (green trace), Acclaim C30 with 1.9 µm (blue trace) and 3.0 µm particle size (yellow trace).

Conflict of interest

Authors declare no conflict of interest.

Acknowledgments

Financial support from the EU H2020 funded project MASSTRPLAN (Grant number 675132; to MF, KC) and German Federal Ministry of Education and Research (BMBF) within the framework of the e:Med research and funding concept for SysMedOS project are gratefully acknowledged. Special thanks to Tabiwang Arrey for scientific support and discussion.

Appendix A. Supplementary data

Supplementary material related to this article can be found, in the online version, at doi:https://doi.org/10.1016/j.chemphyslip.2019.03.006.

References

Bird, S.S., Marur, V.R., Stavrovskaya, I.G., Kristal, B.S., 2012. Separation of cis-trans phospholipid isomers using reversed phase LC with high resolution MS detection. Anal. Chem. 84, 5509–5517. https://doi.org/10.1021/ac300953j.Separation.

Bowden, J.A., Heckert, A., Ulmer, C.Z., Jones, C.M., Koelmel, J.P., Abdullah, L., Ahonen, L., Alnouti, Y., Armando, A.M., Asara, J.M., Bamba, T., Barr, J.R., Bergquist, J., Borchers, C.H., Brandsma, J., Breitkopf, S.B., Cajka, T., Cazenave-Gassiot, A., Checa, A., Cinel, M.A., Colas, R.A., Cremers, S., Dennis, E.A., Evans, J.E., Fauland, A., Fiehn, O., Gardner, M.S., Garrett, T.J., Gotlinger, K.H., Han, J., Huang, Y., Neo, A.H., Hyötyläinen, T., Izumi, Y., Jiang, H., Jiang, H., Jiang, J., Kachman, M., Kiyonami, R., Klavins, K., Klose, C., Köfeler, H.C., Kolmert, J., Koal, T., Koster, G., Kuklenyik, Z., Kurland, I.J., Leadley, M., Lin, K., Maddipati, K.R., McDougall, D., Meikle, P.J., Mellett, N.A., Monnin, C., Moseley, M.A., Nandakumar, R., Oresic, M., Patterson, R., Peake, D., Pierce, J.S., Post, M., Postle, A.D., Pugh, R., Qiu, Y., Quehenberger, O., Ramrup, P., Rees, J., Rembiesa, B., Reynaud, D., Roth, M.R., Sales, S., Schuhmann, K., Schwartzman, M.L., Serhan, C.N., Shevchenko, A., Somerville, S.E., St. John-Williams, L., Surma, M.A., Takeda, H., Thakare, R., Thompson, J.W., Torta, F., Triebl, A., Trötzmüller, M., Ubhayasekera, S.J.K., Vuckovic, D., Weir, J.M., Welti, R., Wenk, M.R., Wheelock, C.E., Yao, L., Yuan, M., Zhao, X.H., Zhou, S., 2017. Harmonizing lipidomics: NIST interlaboratory comparison exercise for lipidomics using SRM 1950–metabolites in frozen human plasma. J. Lipid Res. 58, 2275–2288. https://doi.org/10.1194/jlr.M079012.

Burla, B., Arita, M., Arita, M., Bendt, A.K., Cazenave-Gassiot, A., Dennis, E.A., Ekroos, K., Han, X., Ikeda, K., Liebisch, G., Lin, M.K., Loh, T.P., Meikle, P.J., Orešič, M., Quehenberger, O., Shevchenko, A., Torta, F., Wakelam, M.J.O., Wheelock, C.E., Wenk, M.R., 2018. MS-based lipidomics of human blood plasma: a community-initiated position paper to develop accepted guidelines. J. Lipid Res. https://doi.org/10.1194/jlr.S087163.

Cajka, T., Fiehn, O., 2014. Comprehensive analysis of lipids in biological systems by liquid chromatography-mass spectrometry. Trends Analyt. Chem. 61, 192–206. https://doi.org/10.1016/j.trac.2014.04.017.

Chambers, M.C., MacLean, B., Burke, R., Amodei, D., Ruderman, D.L., Neumann, S., Gatto, L., Fischer, B., Pratt, B., Egertson, J., Hoff, K., Kessner, D., Tasman, N., Shulman, N., Frewen, B., Baker, T.A., Brusniak, M.Y., Paulse, C., Creasy, D., Flashner, L., Kani, K., Moulding, C., Seymour, S.L., Nuwaysir, L.M., Lefebvre, B., Kuhlmann, F., Roark, J., Rainer, P., Detlev, S., Hemenway, T., Huhmer, A., Langridge, J., Connolly, B., Chadick, T., Holly, K., Eckels, J., Deutsch, E.W., Moritz, R.L., Katz, J.E., Agus, D.B., MacCoss, M., Tabb, D.L., Mallick, P., 2012. A cross-platform toolkit for mass spectrometry and proteomics. Nat. Biotechnol. https://doi.org/10.1038/nbt.2377.

Hu, C., Dommelen, J., Van Heijden, R., Van Der, Spijksma, G., Reijmers, T.H., Wang, M., Slee, E., Lu, X., Xu, G., Greef, J., Van Der, Hankemeier, T., van Dommelen, J., van der Heijden, R., Spijksma, G., Reijmers, T.H., Wang, M., Slee, E., Lu, X., Xu, G., van der Greef, J., Hankemeier, T., 2008. RPLC-ion-trap-FTMS method for lipid pro ling of plasma: method validation and application to p53 mutant mouse model. J. Proteome Res. 7, 4982–4991. https://doi.org/10.1021/pr800373m.

Hu, T., Zhang, J.L., 2018. Mass-spectrometry-based lipidomics. J. Sep. Sci. 41, 351–372. https://doi.org/10.1002/jssc.201700709.

IUPAC, 1997. Compendium of chemical terminology. (The "Gold Book), Compiled by A. D. McNaught and A. Wilkinson, 2nd ed. https://doi.org/10.1351/goldbook.T06456.

Lange, M., Ni, Z., Criscuolo, A., Fedorova, M., 2019. Liquid chromatography techniques in

lipidomics research. Chromatographia 82, 77–100. https://doi.org/10.1007/s10337-018-3656-4.
Li, M., Yang, L., Bai, Y., Liu, H., 2014. Analytical methods in lipidomics and their applications. Anal. Chem. 86, 161–175. https://doi.org/10.1021/ac403554h.
Martano, C., Mugoni, V., Dal Bello, F., Santoro, M.M., Medana, C., 2015. Rapid high performance liquid chromatography-high resolution mass spectrometry methodology for multiple prenol lipids analysis in zebrafish embryos. J. Chromatogr. A 1412, 59–66. https://doi.org/10.1016/j.chroma.2015.07.115.
Martin, A.J.P., Synge, R.L.M., 1941. A new form of chromatogram employing two liquid phases 1. Atheory of chromatography 2. Application to the micro - determination of the higher monoamino - acids in proteins. Biochem. J. Lond. 1906 (35), 1358–1368.
Matyash, V., Liebisch, G., Kurzchalia, T.V., Shevchenko, A., Schwudke, D., 2008. Lipid extraction by methyl- tert -butyl ether for high-throughput lipidomics. J. Lipid Res. https://doi.org/10.1194/jlr.D700041-JLR200.
Mayer, S.W., Tompkins, E.R., 1947. Ion Exchange as a separations method. IV. A theoretical analysis of the column separations process. J. Am. Chem. Soc. 69, 2866–2874. https://doi.org/10.1021/ja01203a069.
Narváez-rivas, M., Zhang, Q., 2016. Comprehensive untargeted lipidomic analysis using core – shell C30 particle column and high field orbitrap mass spectrometer. J. Chromatogr. A 1440, 123–134. https://doi.org/10.1016/j.chroma.2016.02.054.
Neue, U.D., 2005. Theory of peak capacity in gradient elution. J. Chromatogr. A 1079, 153–161. https://doi.org/10.1016/j.chroma.2005.03.008.
Ni, Z., Angelidou, G., Lange, M., Hoffmann, R., Fedorova, M., 2017. LipidHunter identifies phospholipids by high-throughput processing of LC-MS and shotgun lipidomics datasets. Anal. Chem. https://doi.org/10.1021/acs.analchem.7b01126.
Ovčačíková, M., Lísa, M., Cífková, E., Holčapek, M., 2016. Retention behavior of lipids in reversed-phase ultrahigh-performance liquid chromatography–electrospray ionization mass spectrometry. J. Chromatogr. A 1450, 76–85. https://doi.org/10.1016/j.chroma.2016.04.082.
Pauling, J.K., Hermansson, M., Hartler, J., Christiansen, K., Gallego, S.F., Peng, B., Ahrends, R., Ejsing, C.S., 2017. Proposal for a common nomenclature for fragment ions in mass spectra of lipids. PLoS One. https://doi.org/10.1371/journal.pone.0188394.
Rainville, P.D., Stumpf, C.L., Shockcor, J.P., Plumb, R.S., Nicholson, J.K., 2007. Novel application of reversed-phase UPLC-oaTOF-MS for lipid analysis in complex biological mixtures: a new tool for lipidomics. J. Proteome Res. https://doi.org/10.1021/pr060611b.
Rampler, E., Criscuolo, A., Zeller, M., El Abiead, Y., Schoeny, H., Hermann, G., Sokol, E., Cook, K., Peake, D.A., Delanghe, B., Koellensperger, G., 2017. A novel lipidomics workflow for improved human plasma identification and quantification using RPLC-MSn methods and isotope dilution strategies. Anal. Chem. https://doi.org/10.1021/acs.analchem.7b05382.
Sandra, K., Pereira, A., dos, S., Vanhoenacker, G., David, F., Sandra, P., 2010. Comprehensive blood plasma lipidomics by liquid chromatography/quadrupole time-of-flight mass spectrometry. J. Chromatogr. A 1217, 4087–4099. https://doi.org/10.1016/j.chroma.2010.02.039.
Shevchenko, A., Simons, K., 2010. Lipidomics: coming to grips with lipid diversity. Nat. Rev. Mol. Cell Biol. https://doi.org/10.1038/nrm2934.
Vyňuchalová, K., Jandera, P., 2015. Comparison of a C30 bonded silica column and columns with shorter bonded ligands in reversed-phase LC. Chromatographia. https://doi.org/10.1007/s10337-015-2899-6.
Witting, M., Maier, T.V., Garvis, S., Schmitt-Kopplin, P., 2014. Optimizing a ultrahigh pressure liquid chromatography-time of flight-mass spectrometry approach using a novel sub-2μm core-shell particle for in depth lipidomic profiling of Caenorhabditis elegans. J. Chromatogr. A 1359, 91–99. https://doi.org/10.1016/j.chroma.2014.07.021.